

1 **Research Article**

2 **Effects of mitochondrial fusion and fission regulation on mouse**  
3 **hippocampal primary cultures: relevance to Alzheimer's disease**

4

5

6 Alina Vadimovna Chaplygina<sup>1, \*</sup>

7 <sup>1</sup> Russian Acad Sci, Inst Cell Biophys, Pushchino 142290, Moscow Oblast, Russia.

8

9

10 **Corresponding author:** Alina Vadimovna Chaplygina

11 **Email:** shadowhao@yandex.ru

12 **Abstract.**

13 **Background:** Alzheimer's disease is a complex disease that begins long before the  
14 first well-known pathophysiological signs appear and requires, among other things,  
15 new diagnostic approaches. This is primarily due to the lack of effective treatment due  
16 to the lack of understanding of the disease mechanisms and the absence of correct  
17 biological models reflecting the cause-and-effect relationships in pathogenesis. One of  
18 the dysfunctional changes in AD is the disruption of mitochondrial fission and fusion  
19 processes.

20 **Methods:** In this study, mitochondrial fusion and fission were regulated in primary  
21 neuro-astrocytic cultures of mouse hippocampus using mitochondrial fission inhibitor,  
22 mitochondrial fusion promoter and exogenous zinc. Changes in mitochondrial and  
23 cellular morphology were assessed, as well as lipofuscin levels as an early marker of  
24 mitochondrial dysfunction. Primary neuro-astrocytic hippocampal cultures of 5xFAD  
25 mice, representing a model of hereditary AD, were used for comparison.

26 **Results:** Use of the mitochondrial fusion promoter converts the mitochondrial  
27 network to a pool of fused mitochondria and results in a drop in neuronal density by  
28 day 5 of exposure with a concomitant drop in astrocyte density by days 1 and 5 of  
29 exposure, accompanied by a drop in lipofuscin fluorescence intensity in culture. The  
30 use of mitochondrial fission inhibitor resulted in the appearance of fused  
31 mitochondria and disappearance of the pool of smallest mitochondria. This was  
32 accompanied by a decrease in neuronal density and an increase in astrocyte density  
33 with a concomitant increase in lipofuscin fluorescence intensity to the level of 5xFAD  
34 culture. Exogenous zinc induces mitochondrial fragmentation and at high  
35 concentrations leads to compensatory astrogliosis and neurodegeneration, while at  
36 low concentrations it decreases lipofuscin fluorescence intensity and affects culture  
37 morphology and changes in astrocyte immunoreactivity to GFAP.

38 **Conclusions:** The study demonstrates that changing the processes of mitochondrial  
39 dynamics affects the morphology of adult cell cultures and can lead to processes  
40 similar to those observed in 5xFAD transgenic cultures.

41 **Keywords:** mitochondria, mitochondrial fusion and fission, 5xFAD, lipofuscin,  
42 Alzheimer's disease, primary hippocampal culture

43

44 **1. INTRODUCTION**

45 Alzheimer's disease (AD) is one of the most common neurodegenerative diseases  
46 associated with impaired cognitive function and progressive neuronal loss. Currently,  
47 researchers have no doubts that mitochondria are involved in the pathogenesis of AD;  
48 moreover, there are hypotheses that place mitochondrial dysfunction in the leading  
49 role in the onset of AD [1,2]. Decreased respiratory capacity, increased mitochondrial  
50 fragmentation, and fractures in mitochondrial cristae structure occur in the brain in  
51 Alzheimer's disease, and abnormalities in mitochondria appear before deposition of  
52 pathologic A $\beta$  plaques [3]. Consistent with the observation that impaired energy  
53 metabolism invariably precedes the clinical onset of Alzheimer's disease,  
54 mitochondrial dysfunction has been established as an early and prominent feature of  
55 the disease [4].

56 Cell functionality is highly dependent on the state of mitochondria, which are  
57 essential for ATP production (general support of cell metabolism) and for maintaining  
58 calcium homeostasis (regulation of neurotransmitters and communication with other  
59 cells). There are different fractions of mitochondria in different parts of the cell at the  
60 same time, performing different functions. These fractions must be in constant  
61 turnover, which maintains the normal physiological state of the cell. This form of  
62 mitochondrial dynamics is known as mitochondrial fission and fusion processes [5].  
63 In normal conditions, mitochondrial fusion and fission occur continuously. A constant  
64 balance is maintained between mitochondria in the fusion-division process, which  
65 deviates from one side to the other in response to the energy and metabolic needs of  
66 the cell.

67 The search for a model of sporadic AD is incomplete, primarily due to the inability to  
68 understand and reproduce the mechanism of disease development. This leads  
69 researchers to the fact that one obvious imbalance process is reproduced on models  
70 (disturbance of balance in the systems of generation and detoxification of reactive  
71 oxygen species in rats of OXYS line [6], mice with surgically removed olfactory  
72 bulbs (olfactory bulbectomized mice) [7] or direct introduction of pathological tau  
73 protein or beta-amyloid into the culture of neurons [8,9].

74 In this work, we wanted to investigate whether disruption of mitochondrial dynamics  
75 in healthy cultures could lead to a process similar to the pathology manifestation in  
76 the 5xFAD mouse line. We directly affect the mitochondrial fusion-division system in  
77 primary mixed neuro-astrocyte hippocampal cultures of mice by inducing shifts

78 toward a prevalence of fusion, or fission. We used primary hippocampal cell culture  
79 of 5xFAD transgenic mice for comparison. Cells in the transgenic culture gradually  
80 accumulate high levels of the neurotoxic agent beta-amyloid from the beginning of  
81 their lives, causing neurodegeneration similar to AD [10]. In addition to the formation  
82 of amyloid plaques, it is characterized by marked astrogliosis and loss of neuronal and  
83 synaptic density, as well as increased levels of lipofuscin, an early marker of cellular  
84 pathology [11]. Alteration of the balance of fusion-division processes in native  
85 primary cell cultures of the hippocampus creates conditions under which an already  
86 adult neuronal culture with no pathologies encounters a forced disturbance of cellular  
87 homeostasis. In 5xFAD mice, it is amyloid overproduction that triggers a cascade of  
88 reactions affecting cellular and subcellular morphology, modeling the typical visible  
89 processes occurring in Alzheimer's disease.

## 90 **2. MATERIALS AND METHODS**

### 91 **2.1 Animal Models**

92 The work was performed on animals that are a model of Alzheimer's disease:  
93 transgenic mice of 5XFAD (TG6799) line and healthy littermates. Cells in the  
94 transgenic culture gradually accumulate high levels of the neurotoxic agent beta-  
95 amyloid, which causes neurodegeneration in AD, from the beginning of their life.  
96 Mice of the 5xFAD line were obtained on a congenic SJL/C57B16 background to  
97 minimize concerns related to allelic segregation and high variability in the original  
98 hybrid background. 5xFAD transgenic mice overexpress the following five FAD  
99 mutations: the APP(695) transgene contains the Swedish (K670N, M671L), Florid  
100 (I716V), and London (V717I) mutations, and the PSEN1 transgene contains the  
101 M146L and L286V mutations. Expression of both transgenes is regulated by murine  
102 Thy1.promoter elements to drive their overexpression specifically in neurons. The  
103 transgenes are inserted at a single locus Chr3:6297836, where they have no effect on  
104 any known genes. Animals were kept in a specialized vivarium with free access to  
105 water and standardized feed at 22 - 24 °C and natural light. The laboratory animals  
106 were treated in accordance with the European Convention for the Protection of  
107 Vertebrates used for experimental and other purposes (Strasbourg, 1986) and the  
108 principles of the Helsinki Declaration (2000). All animal procedures performed with  
109 mice were approved by the Commission on Biosafety and Bioethics (Institute of Cell  
110 Biophysics – Pushchino Scientific Center for Biological Research of the Russian

111 Academy of Sciences) in accordance with Directive 2010/63/EU of the European  
112 Parliament.

113 First, to form groups of animals for breeding, mice were genotyped by classical PCR  
114 using DNA isolated from ear biopsy specimens. The presence of a Tg cassette of 377  
115 bp in length was detected using primers 5'-AGG ACT GAC CAC TCG ACC AG-3'  
116 and 5'-CGG GGG TCT AGT TCT GCA T-3', followed by electrophoretic  
117 visualization.

### 118 **2.1 Primary culture of brain hippocampus.**

119 After genotyping and formation of groups of healthy and 5xFAD animals for breeding,  
120 mice (age 0-1 day) were genotyped to further obtain primary hippocampal cell culture.  
121 For this purpose, the hippocampus was mechanically crushed and treated with  
122 Trypsin-EDTA solution (Gibco, USA). The cell suspension obtained by enzymatic  
123 and mechanical dissociation was then added to the wells of a 12-well plate coated  
124 with Poly-D-Lysine support substrate (Gibco, USA) or to slides, cells were added to 2  
125 or 1 ml of Neurobasal Medium (Gibco, USA) containing 2% B-27 Supplement  
126 (Gibco, USA) and 1% Penicillin-Streptomycin-Glutamine (Gibco, USA), respectively.  
127 Half of the medium was replaced with new medium every five days. Cells were  
128 cultured until the required time in a CO<sub>2</sub> incubator at 37 °C and 5% CO<sub>2</sub>. Thus, we  
129 obtained both control transgenic (Tg) culture and nontransgenic (nTg) culture from  
130 hippocampi of littermate animals. Cultures 14 days old were used in the experiments.  
131 At this term transgenic cultures already well reproduce such characteristic features of  
132 AD as: decrease in neuronal density on the background of increase in astrocyte  
133 density, decrease in the number of synaptic contacts, as well as a significant increase  
134 in the concentration of beta-amyloid.

### 135 **2.3 Regulation of mitochondrial fusion and fission processes.**

136 Two substances with similar functions but different pathways were selected for  
137 mitochondrial fusion shifts. The first substance, Mitochondrial Division Inhibitor 1  
138 (Sigma-Aldrich 475856) (mdivi-1), is a cell-permeable quinazolinone compound that  
139 reversibly inhibits dynamin-like proteins (Drp1) (dynamin-related GTPases)  
140 responsible for mitochondrial fission. The second substance: Mitochondrial Fusion  
141 Promoter M1 (Sigma-Aldrich SML0629) (MFP), is a cell-permeable hydrazone that  
142 enhances mitochondrial fusion and does not affect the morphology of the endoplasmic  
143 network and lysosomes. Preparation of solutions of substances and application into  
144 wells was performed according to the manufacturer's recommendations. In our

145 experiments, we used short (1 day) and long (5 days) observation after Mdivi-1 and  
146 MFP administration to evaluate the response and dynamics of changes in the structure  
147 of the primary hippocampal culture over time.

148 Forcing mitochondrial fission seemed to be a much more difficult task. Currently, the  
149 commercial market cannot provide compounds capable of directly affecting  
150 mitochondrial fission processes. In our experiments we used the introduction of zinc  
151 chloride solution of high (1 $\mu$ M) and low concentration (0.1 $\mu$ M) into the cultures.  
152 "Overloading" the culture cells with zinc causes too much cellular and mitochondrial  
153 stress, which directly affects both mitochondrial and culture morphology, so this  
154 experiment was performed within a single day only. The concentration we chose  
155 allowed for effects on mitochondrial morphology without causing immediate  
156 cytotoxicity, which is primarily reflected in the integrity of the neurite structure. This  
157 experiment reflects short (1 day) and long (5 days) follow-up.

#### 158 **2.4 Visualization of mitochondria.**

159 To visualize mitochondria in cells, we used transduction/transfection of cell cultures  
160 with the CellLight BacMam 2.0 Red system. This ready-to-use construct is  
161 transduced/transfected into cells using BacMam 2.0 technology, where it expresses a  
162 fluorescent protein fused to the E1-alpha-pyruvate dehydrogenase leader sequence. A  
163 suitable volume of reagent is injected into a cell culture of desired density (reagent  
164 calculation is based on the number of cells in the culture according to the  
165 manufacturer's recommendations) and gently mixed. The cells are returned to the  
166 culture incubator overnight, and after approximately 16 hours, the culture is ready for  
167 experiments.

168 Mitochondrial morphology was examined on a Leica DM IL LED microscope (Leica,  
169 Germany) using a x100 oil-immersion objective. We found that fixation of nerve cells  
170 disrupts mitochondrial morphology and triggers an immediate cascade of mitoptosis  
171 reactions with displacement of mitochondrial material together with fluorescent agent  
172 from the cell, which is especially noticeable when working with astrocytes. Therefore,  
173 all data on mitochondrial morphology were obtained on live, unfixed cell cultures.

#### 174 **2.5 Detection of intracellular lipofuscin**

175 We also used spectrofluorimetric detection of lipofuscin, an autofluorescent aging  
176 pigment, as a marker of changes in cellular metabolism. For this purpose, culture  
177 plates with primary hippocampal cultures were washed three times from the medium  
178 with PBS and poured into a solution of 5% sodium dodecyl sulfate in water for 5

179 minutes with simultaneous stirring on a shaker equipped with a refrigerant, which  
180 allowed to completely destroy cell cultures and transfer them into solution. The  
181 resulting suspensions were frozen and further used for experiments. Sodium dodecyl  
182 sulfate, disintegrates protein complexes, destroying cell membranes, but does not  
183 destroy lipofuscin, due to its N-substituted imines - Schiff bases. The addition of  
184 detergent in our experiments, in addition to chemical dissociation, reduced light  
185 scattering and eliminated the effect of Tyndall-Rayleigh hypochromism, directly  
186 affecting the registration of spectral characteristics.

187 Protein concentration in the obtained suspensions was determined and equilibrated by  
188 the Lowry method and UV-express method by the optical density of tryptophan  
189 protein in ultraviolet at 286 nm [12]. UV spectroscopy methods are based on the  
190 ability of solutions to absorb light at around 280 nm due to the presence of the amino  
191 acids' tryptophan, tyrosine and phenylalanine in proteins. The detection results are  
192 directly proportional to the content of these amino acids in proteins. To obtain reliable  
193 and accurate results, the optical density values of the solutions must meet the  
194 requirements of linearity over the range of protein concentrations to be determined.

195 Lipofuscin formation was detected by a characteristic fluorescence band at about 450  
196 nm under excitation at a wavelength of 360 nm. Lipofuscin content in homogenates  
197 was determined on a Perkin Elmer MPF-44B spectrofluorimeter (USA) in multiway  
198 mirror microcuvettes for measuring fluorescence of weakly absorbing solutions. The  
199 cuvettes provide multiple enhancement of fluorescence intensity due to the increased  
200 optical path length of the excitation light and the added light collection of the  
201 emission. Excitation light entering through a narrow window in the frontal mirror wall  
202 of the cuvette passes through the solution and onto the mirror opposite side, is  
203 deflected and undergoes two or three reflections within the cuvette. The radiation is  
204 collected at right angles. Additional light collection of radiation is provided by a  
205 mirror side wall that directs the fluorescence into the registration channel. When it is  
206 used, light losses and artifact polarization are minimal compared to a conventional  
207 cuvette located near concave mirrors.

## 208 **2.6 Immunocytochemistry**

209 For immunocytochemical staining for neuronal and astrocyte markers, cell cultures  
210 were fixed for 10 minutes with 4% paraformaldehyde. Membrane permeability was  
211 then increased using 0.2% Triton X-100 solution and nonspecific binding to antigens  
212 was blocked for one hour at room temperature in PBST (PBS+0.1% Tween 20) + 1%

213 BSA solution using 10% normalized donkey serum (Abcam, ab7475) and 5%  
214 normalized goat serum (Invitrogen, 31872). Cultures were left overnight at 4 °C for  
215 incubation with primary antibodies. After incubation with primary antibodies, binding  
216 was performed with appropriate secondary antibodies conjugated to fluorescent tags  
217 for 2 hours at room temperature. After each treatment, cells were washed 3 times with  
218 PBS solution (pH 7.4) for 5 minutes each. The following primary and secondary  
219 antibodies were used to stain for neurons - Anti-MAP2 antibody (ab32454, 1:200) and  
220 corresponding Alexa594nm (ab150080, 1:400); astrocytes - Anti-GFAP antibody  
221 (ab4674, 1:800); Alexa488nm (ab150169, 1:1000).

## 222 **2.7 Statistical Analysis**

223 Statistical analysis of the results was performed using Sigma Plot 12.5 software. Data  
224 are presented as mean and standard error of mean for visual convenience. The  
225 hypothesis of normal distribution was tested using the Shapiro-Wilk test. One-factor  
226 ANOVA analysis of variance with a posteriori comparison of groups using Dunn's  
227 and Bonferroni methods were used to compare differences between groups and to  
228 determine statistical significance.

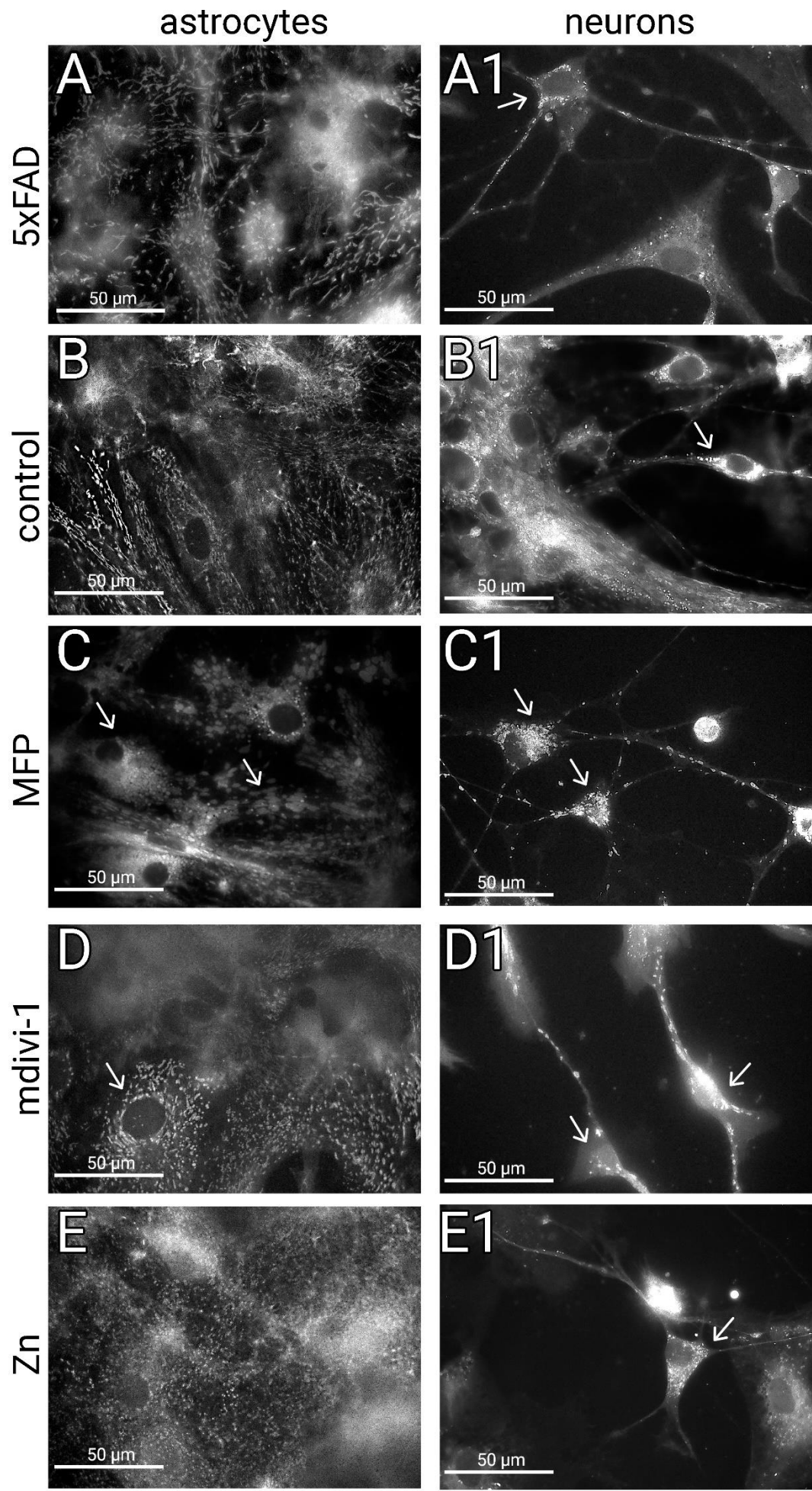
## 229 **3. RESULTS**

### 230 **3.1 Forced activation of mitochondrial fusion leads to slow degradation of the** 231 **culture.**

232 Utilization of the mitochondrial fusion promoter M1 (MFP) in astrocytes converts the  
233 mitochondrial network into a pool of fused and hyperfused mitochondria (**Figure 1 C**).  
234 A similar pattern is observed in neurons, in which fused mitochondria become like  
235 elongated sticks or become large fused mitochondria (**Figure 1, C1**). **Figure 2, B-B1**  
236 is a tendency for neuronal density to fall by day 1 of exposure, and it falls  
237 significantly relative to the control native culture level by day 5 ( $47.4 \pm 1$  at native  
238 level,  $36.7 \pm 1.4$  at day 5,  $p < 0.05$ , one-way ANOVA followed by Dunn's post-tests).  
239 There was a decrease in astrocytic density by day 1 ( $52,3 \pm 1$  in control,  $48,6 \pm 1.6$  at  
240 day 1,  $p < 0.05$ , one-way ANOVA followed by Dunn's post-tests), and a further  
241 progressive decrease in density by day 5 ( $37.9 \pm 1,5$  at day 5,  $p < 0.05$ , one-way  
242 ANOVA followed by Dunn's post-tests). We also observe an interesting effect of  
243 decreasing lipofuscin fluorescence by day 1 ( $345 \pm 2$  in native levels,  $277 \pm 2$  at day 1,  
244  $p < 0.001$  one-way ANOVA followed by Dunn's post-tests) and day 5 ( $131 \pm 1,5$ ,  
245  $p < 0.001$  one-way ANOVA followed by Dunn's post-tests) of fusion activator



246 exposure at **Figure 3, B**. Overall, prolonged exposure to MFP resembles a depletion  
247 of internal culture resources.



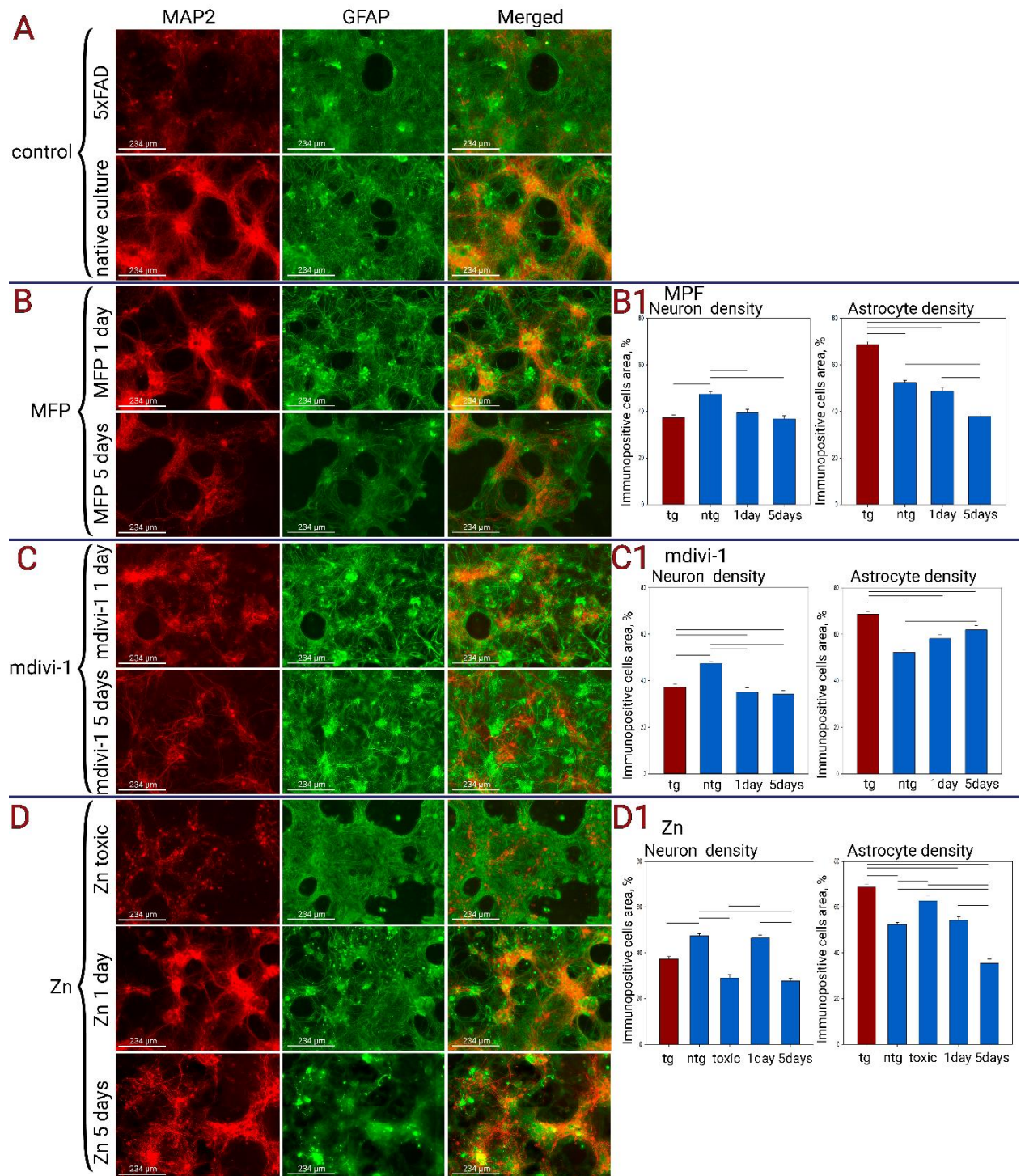
249 **Figure 1.** *Alteration of mitochondrial morphology under the action of different fusion*  
250 *and fission modulators. Mitochondria staining was performed by*  
251 *transfection/transduction with the CellLight BacMam 2.0 system. Mitochondrial*  
252 *morphology was examined on a Leica DM IL LED microscope using a x100 oil-*  
253 *immersion objective. A - mitochondrial network with a tendency to mitochondrial*  
254 *fusion in 5xFAD astrocytes. A1 - mitochondria with a tendency to reduce their size in*  
255 *the neuron of cultures of 5xFAD mice (arrow indicates the body of the neuron). B -*  
256 *Mitochondrial network in healthy astrocytes, has more elongated mitochondria. B1 -*  
257 *Neurons in healthy cultures, you can see mitochondria of different sizes (arrow*  
258 *indicates the body of the neuron). C - Mitochondria under the action of MFP in*  
259 *astrocytes fuse into grouped round (fused) or hyperfused mitochondria. Bright*  
260 *examples are indicated by the arrow. C1 - Mitochondria in neurons become larger*  
261 *under the action of MFP (arrow indicates neuron bodies). D - Mitochondria in*  
262 *astrocytes under the action of mdivi-1 lose the shape of the mitochondrial network*  
263 *and the number of smallest mitochondria also decreases. D1 - Mitochondria in*  
264 *neurons under the influence of mdivi-1 become larger, the smallest mitochondria*  
265 *disappear (arrow indicates neuron bodies). E - Mitochondria in astrocytes under the*  
266 *action of zinc completely lose the shape of the network. E1 - Mitochondria in neurons*  
267 *under the action of zinc become small (arrow indicates neuron bodies).*

268

### 269 **3.2 Inhibition of mitochondrial fission makes the culture similar to that of** 270 **5xFAD.**

271 Morphologically, the use of the mitochondrial fission inhibitor mdivi-1 resulted in  
272 larger mitochondria being found in neuron bodies and neurites. At the same time, in  
273 astrocytes there was fragmentation of the mitochondrial network and instead fused  
274 mitochondria were found in greater numbers. We also observed a decrease in the pool  
275 of smallest mitochondria, which almost completely disappeared in astrocytes and  
276 remained only in neurons (**Figure 1, D-D1**). After one day of mitochondrial fission  
277 inhibition, neuronal density decreased relative to the control group ( $47,4 \pm 1$  at native  
278 level,  $35 \pm 2$  at day 1,  $p < 0.05$ , one-way ANOVA followed by Dunn's post-tests) and  
279 did not decrease further by day 5. There was an increase in astrocytic density by day 1,  
280 and by day 5 ( $52,3 \pm 1.2$  at native level,  $58,2 \pm 1,7$  at day 1,  $68,1 \pm 1,8$  at day 5,  $p < 0.05$ ,  
281 one-way ANOVA followed by Dunn's post-tests). In addition, there was a significant  
282 increase in lipofuscin fluorescence correlating with the time of mdivi-1 exposure

283 **(Figure 3, C)**. Moreover, by day 5 of mitochondrial fission inhibition, the intensity of  
 284 lipofuscin fluorescence increased such that it was not significantly different from  
 285 lipofuscin fluorescence in transgenic culture ( $571 \pm 3$  in Tg culture,  $571 \pm 2$  at day 5  
 286  $p < 0.001$  one-way ANOVA followed by Bonferroni post-tests). Thus, inhibition of  
 287 mitochondrial fission in healthy cultures leads to a cascade of events reminiscent of  
 288 those in transgenic culture (**Figure 2, C**).



289

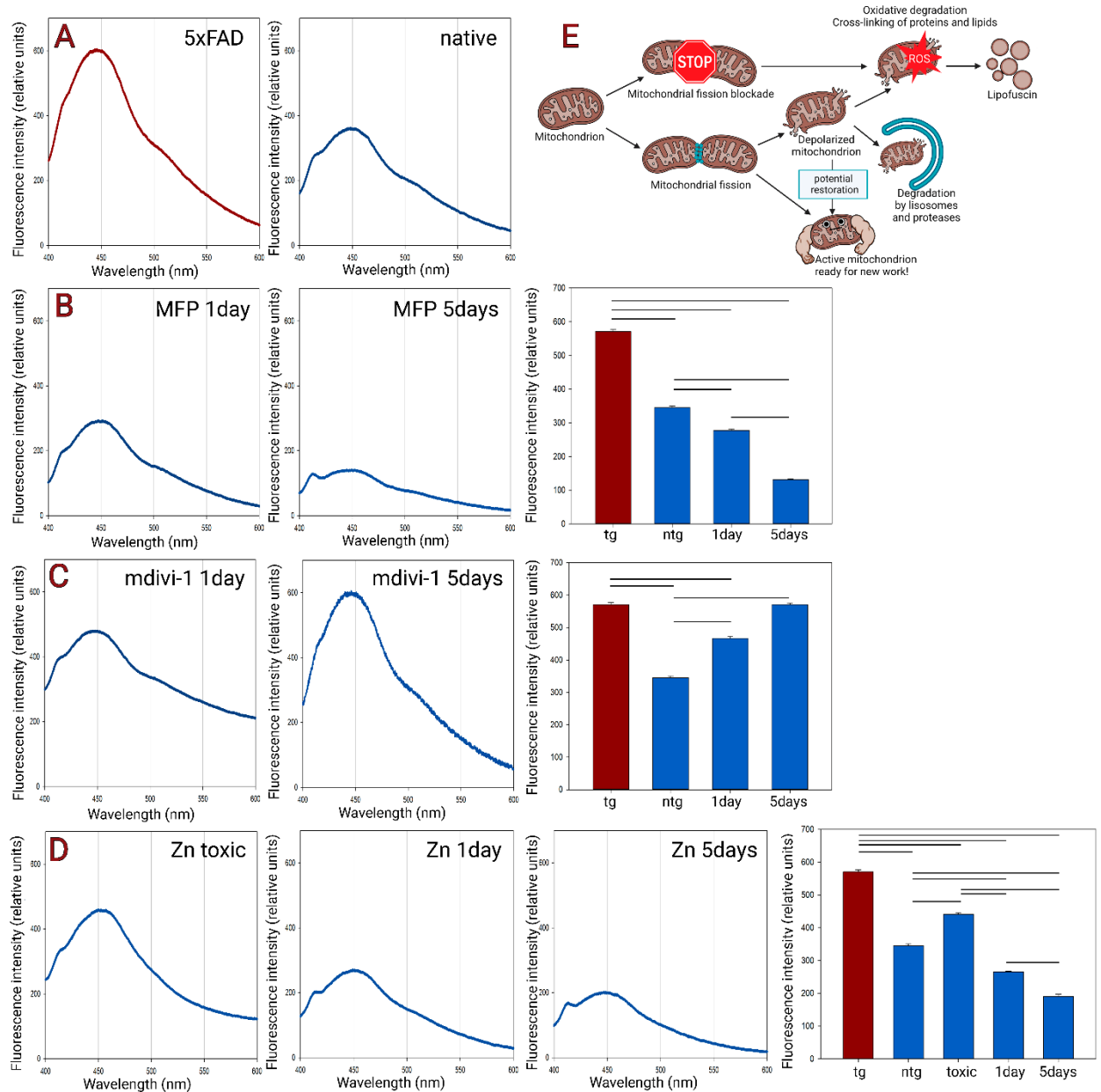
290 **Figure 2.** Immunopositivity to an astrocyte marker (GFAP in green) and a neuronal  
291 marker (MAP2 in red) in primary neuronal cultures under the influence of fusion and  
292 fission activators. A - Control transgenic 5xFAD culture that served as a reference for  
293 modeling pathogenesis and control healthy culture. B - Effect of MFP on culture  
294 morphology after 1 and 5 days of administration. B1 - Neuronal and astrocytic  
295 densities (in %) under the effect of MFP. C - Effect of mdivi-1 on culture morphology  
296 after 1 and 5 days of administration. C1 - Neuronal and astrocytic densities (in %)  
297 under the effect of mdivi-1. D1 - Effect of Zn on culture morphology after 1 and 5  
298 days of administration. D1 - Neuronal and astrocytic densities (in %) under the effect  
299 of Zn.

300

### 301 **3.3 Exogenous zinc induces mitochondrial fission, alters cell culture morphology** 302 **and induces GFAP aggregation.**

303 We used exogenous zinc chloride solution to modulate mitochondrial fission. In this  
304 case, zinc overload at high, rather uncomfortable concentrations for nerve cells,  
305 induces cellular and mitochondrial stress affecting mitochondrial morphology, which  
306 is consistent with the results of [13]. Primary culture neurons are the first to suffer  
307 from zinc overload, at the same time in culture it was observed compensatory  
308 astrogliosis (**Figure 2, D**). Treatment of cultures with excessive zinc resulted in  
309 neurite destruction and a drop in neuronal density relative to control cultures ( $47,4 \pm 1$   
310 in native,  $29 \pm 1,5$  under toxic influence,  $p < 0.001$ , one-way ANOVA followed by  
311 Dunn's post-tests), while there was a strong compensatory astrocyte overgrowth  
312 ( $52,38 \pm 1$  in native,  $62,7 \pm 2,2$  under toxic influence,  $p < 0.001$ , one-way ANOVA  
313 followed by Dunn's post-tests) and an increase in lipofuscin fluorescence intensity  
314 (**Figure 3, D**) ( $344,9 \pm 2,7$  in native,  $440 \pm 1,2$  under toxic influence,  $p < 0.05$  one-way  
315 ANOVA followed by Dunn's post-tests). Using lower concentrations of zinc chloride  
316 solution allowed us to achieve the same morphologically detectable mitochondrial  
317 fission (**Figure 1, E-E1**), in which neurites do not receive such a high zinc overload  
318 (**Figure 2, D**). Low zinc concentrations caused no significant change in neuronal and  
319 astrocytic density by day 1, but reduced lipofuscin fluorescence intensity ( $265 \pm 1$  at  
320 day 1,  $p < 0.05$  one-way ANOVA followed by Dunn's post-tests). However, on day 5  
321 (**Figure 2, D1**) of the experiment, a fall in neuronal density was already again  
322 observed ( $47,4 \pm 1$  at native,  $27,7 \pm 1,3$  at day 5,  $p < 0.001$ , one-way ANOVA followed  
323 by Dunn's post-tests) with a concomitant drop in astrocyte density ( $52,3 \pm 1$  at native,

324 35,4±1,8 at day 5,  $p < 0.001$ , one-way ANOVA followed by Dunn's post-tests), and  
 325 the cluster morphology of the culture was impaired, neurons became less likely to  
 326 assemble into clustered structures, and began to show altered immunoreactivity to  
 327 glial fibrillary acidic protein, and pathologic aggregation of GFAP increased, however,  
 328 lipofuscin fluorescence intensity was still reduced ( $190 \pm 3$  at day 5,  $p < 0.05$  one-way  
 329 ANOVA followed by Dunn's post-tests).



330  
 331 **Figure 3.** Emission spectra of lipofuscin fluorescence (360/450) and fluorescence  
 332 intensity at the maximum point. A - Fluorescence emission spectra in 5xFAD  
 333 hippocampal cultures and healthy cultures. B - Effect of MFP on lipofuscin  
 334 fluorescence intensity. C - Effect of mdivi-1 on lipofuscin fluorescence intensity. D -

335 *Effect of Zn on the intensity of lipofuscin fluorescence. E - Suggested mechanism of*  
336 *lipofuscin formation from mitochondria.*

337

#### 338 **4. DISCUSSION**

339 Normal mitochondrial fusion and fission dynamics is the basis for maintaining a  
340 healthy mitochondrial pool also through mitophagy, the disruption of which leads to  
341 the degradation of mitochondria into lipofuscin granules [14].

342 First, we would like to talk about lipofuscin. It is a substance consisting of oxidized  
343 lipids, covalently cross-linked proteins, oligosaccharides and metals [15]. The  
344 composition of lipofuscin is largely dependent on the intracellular site of action of  
345 reactive oxygen species on proteins and lipids. Lipofuscin accumulation is directly  
346 proportional to pathologies of various genesis and also increases under conditions of  
347 oxidative stress and reactive oxygen species produced by damaged mitochondria  
348 (**Figure 2, E**). Although, lipofuscin is thought to be a marker of senescent cells, recent  
349 work shows its close association with pathologic tau protein and A $\beta$  in AD [16,17].  
350 Moreover, a new study, shows that  $\alpha$ -structured protein lipofuscin is a toxic  
351 component of  $\beta$ -structured amyloid plaques [18]. Since lipofuscin has the property of  
352 autofluorescence, it can be used as a marker of disorders even before the first  
353 morphologic manifestations. That said, one of the most frequent descriptions of  
354 lipofuscin sounds like "intracellular trash". This term denotes one of the interesting  
355 properties of lipofuscin - extreme resistance to cellular proteolysis, which is explained  
356 by "cross-linking" of aldehyde and amino groups of the peptide to form stable  
357 polymeric structures.

358 We see that the accumulation of lipofuscin in our experiments occurs in two cases.  
359 The first is the toxic effect of high concentrations of exogenous zinc, which is quite  
360 explained by the activation of peroxidation and, in general, quite a common pathway  
361 of lipofuscin increase. The second is inhibition of mitochondrial fission. Thus, by day  
362 5 of fission inhibition, the fluorescence intensity of lipofuscin in the experimental  
363 groups is compared to control 5xFAD transgenic animals. The issue [19] states that  
364 the normal mitochondrial fission cycle involves the formation of two daughter  
365 mitochondria, one of which has a higher membrane potential and goes on to the  
366 fusion-fission cycle, and the other, with a more depolarized membrane, remains  
367 separated until membrane potential is restored or until elimination by autophagy. And  
368 we can assume that the increase in lipofuscin in this case is a process of accumulation

369 of intracellular debris associated with insufficient mitochondrial division and  
370 clearance. And therefore, activation of fission by non-toxic concentrations of zinc,  
371 although leading to deleterious effects in culture, decreased the level of lipofuscin. At  
372 the same time, the activation of mitochondrial fusion, although leading to the  
373 degradation of the culture, did not lead to the formation of lipofuscin. On the contrary,  
374 it decreased over time. This can be taken to mean that by acting on the fusion  
375 promoter, we are not blocking fission, and mitochondria still have the ability to  
376 maintain fission dynamics. Also, given the close relationship between lipofuscin and  
377 peroxidation, we can assume that when mitochondria fuse, cells are not subjected to  
378 oxidative stress.

379 It has been reported that 5xFAD transgenic mice and a reproducible neuro-astrocytic  
380 culture from them, which we considered as a control, already have a shift in  
381 mitochondrial balance toward excess fission [20]. Also, loss of the central  
382 mitochondrial fission protein dynamin-related mitochondrial fission protein 1 (Drp1)  
383 increases the toxicity of mutant APP in vivo [21]. In the 5xFAD mouse model, all  
384 mutations target the hyperproduction of human A $\beta$ 1-42 [22], it is the overproduction  
385 of toxic agents that is the cause of dysfunction in this model. We assume that the  
386 increased mitochondrial fission in this model is secondary and is related to the fact  
387 that the cells are trying to get rid of toxic amyloid in this way. In our experiments,  
388 inhibition of mitochondrial fission resulted in a cascade of reactions characteristic of  
389 5xFAD culture. In addition to a pathologic increase in lipofuscin, we observed a  
390 decrease in neuronal density and compensatory overgrowth of astroglia, which within  
391 this model can be considered as a manifestation of astrogliosis. That is, cellular toxin  
392 accumulation and mitochondrial fission mediate each other.

393 At the same time activation of cell division did not lead to such consequences. But we  
394 can assume that zinc is a toxic agent in general and its mechanism of operation is a  
395 reflection of how the introduction of an external toxic agent (similar to A $\beta$ 1-42  
396 expression in 5xFAD) leads to an attempt of mitochondria to clean themselves and the  
397 cell from contaminants.

398 In doing so, the prolonged action of the fusion promoter resembles the depletion of  
399 internal resources in a healthy culture. This process of slow degeneration is broadly  
400 similar to what one pathway of cell culture degeneration looks like. It loses clustering  
401 and shrinks (although in general there is another pathway of culture degradation,  
402 abrupt neurosphere clustering, where thin neuro-astrocytic strands stretch between



403 densely packed neurospheres, linking them to other neurospheres, this is characteristic  
404 of primary cultures with high initial stem cell content or their increased level of  
405 activity). Mitochondria fusion is thought to result in enhanced ATP energy supply to  
406 cells because they have more cristae, increased levels of dimerization and ATP  
407 synthase activity and support ATP synthesis [23,24]. However, excess ATP leads to  
408 neuronal dysfunction and death [25] and is a prerequisite for the realization of the  
409 cellular apoptosis cascade [26]. In this case, the mitochondria resulting from fusion  
410 may be too large for mitochondrial transport. We find it difficult to say what the  
411 mechanism of culture degeneration is in this case. However, the absence of oxidative  
412 stress and the drop in lipofuscin levels shows that this process is more likely a  
413 controlled extinction of activity rather than an abrupt pathology. It can be stated  
414 unequivocally that only harmonious functioning of this system can ensure normal  
415 physiological functions of mitochondria, and any shift to one side of the dynamic  
416 process leads to disorders.

417

## 418 **5. CONCLUSIONS**

419 Forced alteration of mitochondrial fusion and fission leads to morphologic changes in  
420 primary neuro-astrocytic cultures of mouse hippocampus. Activation of mitochondrial  
421 fusion leads to slow depletion of the culture in the absence of visible degenerative  
422 processes and oxidative stress. Inhibition of mitochondrial fission leads to a cascade  
423 of events reminiscent of those occurring in a culture of 5xFAD animals (a genetic  
424 model of AD) - astrogliosis, decreased neuronal density, and increased lipofuscin  
425 levels. Exogenous zinc induces mitochondrial fission and provokes compensatory  
426 astrogliosis at toxic concentrations, and at lower concentrations leads to a slow  
427 decrease in culture clustering, changes in astrocyte immunoreactivity to GFAP and its  
428 aggregation, whereas lipofuscin fluorescence was still decreased. We suggest that  
429 mitochondrial fission in models with toxic mitochondrial damage is a compensatory  
430 process in which mitochondria strive to clear the cell of toxic agents, but which may  
431 lead to a cascade of reactions that provoke further development of pathologies.

432

## 433 **6. DECLARATION**

### 434 **Acknowledgments**

435 The authors extend their appreciation to V.I. Kovalev for constructive feedback  
436 during the preparation of the manuscript.

437 **Authors' contributions**

438 The authors contributed equally to the preparation of the study.

439 **Availability of data and materials**

440 The results of the work can be found at the google link. Or write to the corresponding  
441 author.

442 *<https://docs.google.com/spreadsheets/d/1qnVotSWUwWIXUEAVkRCA3HBqfkvMVetg/edit?usp=sharing&oid=105509595749562341769&rtpof=true&sd=true>*

444 **Financial support and sponsorship**

445 This work was supported by the Russian Science Foundation (RSF), project No. 23-  
446 25-00485.

447 **Conflicts of interest**

448 All authors declared that there are no conflicts of interest.

449 **Ethical approval and consent to participate**

450 The laboratory animals were treated in accordance with the European Convention for  
451 the Protection of Vertebrates used for experimental and other purposes (Strasbourg,  
452 1986) and the principles of the Helsinki Declaration (2000). All animal procedures  
453 performed with mice were approved by the Commission on Biosafety and Bioethics  
454 (Institute of Cell Biophysics – Pushchino Scientific Center for Biological Research of  
455 the Russian Academy of Sciences) in accordance with Directive 2010/63/EU of the  
456 European Parliament.

457

458 **REFERENCES**

- 459 [1] Wang W, Zhao F, Ma X, Perry G, Zhu X. Mitochondria Dysfunction in the  
460 Pathogenesis of Alzheimer's Disease: Recent Advances. *Molecular*  
461 *Neurodegeneration*, 2020, 15(1): 30.
- 462 [2] Peng Y, Gao P, Shi L, Chen L, Liu J, Long J. Central and Peripheral  
463 Metabolic Defects Contribute to the Pathogenesis of Alzheimer's Disease: Targeting  
464 Mitochondria for Diagnosis and Prevention. *Antioxidants & Redox Signaling*, 2020,  
465 32(16): 1188–1236.
- 466 [3] Sorrentino V, Romani M, Mouchiroud L, Beck JS, Zhang H, D'Amico D,  
467 Moullan N, Potenza F, Schmid AW, Rietsch S, Counts SE, Auwerx J. Enhancing  
468 Mitochondrial Proteostasis Reduces Amyloid- $\beta$  Proteotoxicity. *Nature*, 2017,  
469 552(7684): 187–193.
- 470 [4] Wang X, Wang W, Li L, Perry G, Lee H, Zhu X. Oxidative Stress and  
471 Mitochondrial Dysfunction in Alzheimer's Disease. *Biochimica et Biophysica Acta*  
472 *(BBA) - Molecular Basis of Disease*, 2014, 1842(8): 1240–1247.
- 473 [5] Archer SL. Mitochondrial Dynamics--Mitochondrial Fission and Fusion in  
474 Human Diseases. *The New England Journal of Medicine*, 2013, 369(23): 2236–2251.
- 475 [6] Stefanova NA, Kozhevnikova OS, Vitovtov AO, Maksimova KY, Logvinov S  
476 V, Rudnitskaya EA, Korbolina EE, Muraleva NA, Kolosova NG. Senescence-  
477 Accelerated OXYS Rats: A Model of Age-Related Cognitive Decline with Relevance  
478 to Abnormalities in Alzheimer Disease. *Cell Cycle (Georgetown, Tex.)*, 2014, 13(6):  
479 898–909.
- 480 [7] Avetisyan A V, Samokhin AN, Alexandrova IY, Zinovkin RA, Simonyan RA,  
481 Bobkova N V. Mitochondrial Dysfunction in Neocortex and Hippocampus of  
482 Olfactory Bulbectomized Mice, a Model of Alzheimer's Disease. *Biochemistry.*  
483 *Biokhimiia*, 2016, 81(6): 615–623.
- 484 [8] Calkins MJ, Manczak M, Mao P, Shirendeb U, Reddy PH. Impaired  
485 Mitochondrial Biogenesis, Defective Axonal Transport of Mitochondria, Abnormal  
486 Mitochondrial Dynamics and Synaptic Degeneration in a Mouse Model of  
487 Alzheimer's Disease. *Human Molecular Genetics*, 2011, 20(23): 4515–4529.
- 488 [9] Zhang L, Trushin S, Christensen TA, Tripathi U, Hong C, Geroux RE, Howell  
489 KG, Poduslo JF, Trushina E. Differential Effect of Amyloid Beta Peptides on  
490 Mitochondrial Axonal Trafficking Depends on Their State of Aggregation and  
491 Binding to the Plasma Membrane. *Neurobiology of Disease*, 2018, 114: 1–16.

- 492 [10] Bilkei-Gorzo A. Genetic Mouse Models of Brain Ageing and Alzheimer's  
493 Disease. *Pharmacology & Therapeutics*, 2014, 142(2): 244–257.
- 494 [11] AUTHOR'S ARTICLE, 2023.
- 495 [12] AUTHOR'S ARTICLE 2018.
- 496 [13] Knies KA, Li Y V. Zinc Cytotoxicity Induces Mitochondrial Morphology  
497 Changes in Hela Cell Line. *International Journal of Physiology, Pathophysiology and*  
498 *Pharmacology*, 2021, 13(2): 43–51.
- 499 [14] Rodolfo C, Campello S, Cecconi F. Mitophagy in Neurodegenerative Diseases.  
500 *Neurochemistry International*, 2018, 117: 156–166.
- 501 [15] Kikugawa K, Kato T, Beppu M, Hayasaka A. Fluorescent and Cross-Linked  
502 Proteins Formed by Free Radical and Aldehyde Species Generated during Lipid  
503 Oxidation. *Advances in Experimental Medicine and Biology*, 1989, 266: 345–56;  
504 discussion 357.
- 505 [16] Dehkordi SK, Walker J, Sah E, Bennett E, Atrian F, Frost B, Woost B,  
506 Bennett RE, Orr TC, Zhou Y, Andhey PS, Colonna M, Sudmant PH, Xu P, Wang M,  
507 Zhang B, Zare H, Orr ME. Profiling Senescent Cells in Human Brains Reveals  
508 Neurons with CDKN2D/P19 and Tau Neuropathology. *Nature Aging*, 2021, 1(12):  
509 1107–1116.
- 510 [17] Moreno-García A, Kun A, Calero O, Medina M, Calero M. An Overview of  
511 the Role of Lipofuscin in Age-Related Neurodegeneration. *Frontiers in Neuroscience*,  
512 2018, 12: 464.
- 513 [18] Serwer P, Wright ET, Hunter B. Additions to Alpha-Sheet Based Hypotheses  
514 for the Cause of Alzheimer's Disease. *Journal of Alzheimer's Disease: JAD*, 2022,  
515 88(2): 429–438.
- 516 [19] Liesa M, Shirihai OS. Mitochondrial Dynamics in the Regulation of Nutrient  
517 Utilization and Energy Expenditure. *Cell Metabolism*, 2013, 17(4): 491–506.
- 518 [20] Wang L, Guo L, Lu L, Sun H, Shao M, Beck SJ, Li L, Ramachandran J, Du Y,  
519 Du H. Synaptosomal Mitochondrial Dysfunction in 5xFAD Mouse Model of  
520 Alzheimer's Disease. *PloS One*, 2016, 11(3): e0150441.
- 521 [21] Shields LY, Li H, Nguyen K, Kim H, Doric Z, Garcia JH, Gill TM, Haddad D,  
522 Vossel K, Calvert M, Nakamura K. Mitochondrial Fission Is a Critical Modulator of  
523 Mutant APP-Induced Neural Toxicity. *The Journal of Biological Chemistry*, 2021,  
524 296: 100469.
- 525 [22] Ismeurt C, Giannoni P, Claeysen S. Chapter 13 - The 5xFAD Mouse Model of

526 Alzheimer's Disease. In: Martin CR, Preedy VR (eds). *Diagnosis Manag. Dement.*  
527 Academic Press 2020; 207–221.

528 [23] Hoitzing H, Johnston IG, Jones NS. What Is the Function of Mitochondrial  
529 Networks? A Theoretical Assessment of Hypotheses and Proposal for Future  
530 Research. *BioEssays : News and Reviews in Molecular, Cellular and Developmental*  
531 *Biology*, 2015, 37(6): 687–700.

532 [24] Gomes LC, Di Benedetto G, Scorrano L. During Autophagy Mitochondria  
533 Elongate, Are Spared from Degradation and Sustain Cell Viability. *Nature Cell*  
534 *Biology*, 2011, 13(5): 589–598.

535 [25] Pontes MH, Sevostyanova A, Groisman EA. When Too Much ATP Is Bad for  
536 Protein Synthesis. *Journal of Molecular Biology*, 2015, 427(16): 2586–2594.

537 [26] Zamaraeva M V, Sabirov RZ, Maeno E, Ando-Akatsuka Y, Bessonova S V,  
538 Okada Y. Cells Die with Increased Cytosolic ATP during Apoptosis: A  
539 Bioluminescence Study with Intracellular Luciferase. *Cell Death and Differentiation*,  
540 2005, 12(11): 1390–1397.

541